Article

Not peer-reviewed version

Chimeric Anti-Glypican 1 Antibodies Exert Antitumor Activities in Xenograft Models of Lung and Pancreatic Cancers

Haruto Yamamoto , Hiroyuki Suzuki * , Tomokazu Ohishi , Hiroyuki Satofuka , Mika K. Kaneko , Yukinari Kato *

Posted Date: 13 February 2026

doi: 10.20944/preprints202602.1130.v1

Keywords: Glypican-1; monoclonal antibody therapy; ADCC; CDC; lung cancer; pancreatic cancer

 doi:10.20944/preprints202602.1130.v1

Article

Chimeric Anti-Glypican 1 Antibodies Exert Antitumor Activities in Xenograft Models of Lung and Pancreatic Cancers

Haruto Yamamoto [1,†], Hiroyuki Suzuki [1,*,†], Tomokazu Ohishi [2,†], Hiroyuki Satofuka [1], Mika K. Kaneko [1] and Yukinari Kato [1,*]

[1] Department of Antibody Drug Development, Tohoku University Graduate School of Medicine, 2-1 Seiryo-machi, Aoba-ku, Sendai, Miyagi 980-8575, Japan

[2] Institute of Microbial Chemistry (BIKAKEN), Laboratory of Oncology, Microbial Chemistry Research Foundation, 3-14-23 Kamiosaki, Shinagawa-ku, Tokyo 141-0021, Japan

* Correspondence: hiroyuki.suzuki.b4@tohoku.ac.jp (H. S.); yukinari.kato.e6@tohoku.ac.jp (Y.K.); Tel.: +81-22-717-8207

† Contributed equally to this work.

Abstract

Glypican-1 (GPC1) has emerged as a critical mediator of malignant tumor progression. GPC1 plays essential roles in regulating various signaling pathways involved in tumor cell proliferation, invasiveness, and tumorigenesis. Overexpression of GPC1 in tumors mediates oncogenic transformation, epithelial-to-mesenchymal transition, metastatic dissemination, and therapeutic resistance. Accordingly, GPC1-targeted therapeutic strategies have been investigated in clinical and preclinical studies. However, the clinical efficacy has been limited. We previously developed an anti-GPC1 monoclonal antibody (mAb), G$_1$Mab-28 (mouse IgG$_1$, κ), which exhibits high affinity and specificity for GPC1. In the present study, we generated recombinant isotype-converted G$_1$Mab-28, including G$_1$Mab-28-mG$_{2a}$ (mouse IgG$_{2a}$) and G$_1$Mab-28-hG$_1$ (human IgG$_1$). Both mAbs recognized GPC1-expressing human tumor cell lines, including lung squamous cell carcinoma PC10 and pancreatic ductal adenocarcinoma PK-45H, by flow cytometry. Moreover, both mAbs exerted antibody-dependent cellular cytotoxicity and complement-dependent cytotoxicity against those cell lines. In mouse xenograft models, treatment with the mAbs resulted in potent antitumor efficacy against PC10 and PK-45H tumors. Collectively, these findings support the therapeutic potential of G$_1$Mab-28 for the treatment of GPC1-positive tumors.

Keywords: Glypican-1; monoclonal antibody therapy; ADCC; CDC; lung cancer; pancreatic cancer

1. Introduction

Glypican-1 (GPC1) is an extracellular matrix-associated heparan sulfate (HS) proteoglycan and serves as a co-receptor for fibroblast growth factors, hepatocyte growth factor, some Wnt ligands, and TGF-β to enhance the signaling pathways. GPC1 plays essential roles in tumor cell proliferation, invasiveness, epithelial-to-mesenchymal transition, stemness, and therapeutic resistance.[1–3] Overexpression of GPC1 is significantly associated with reduced overall survival, disease-free survival, and/or relapse-free survival in esophageal squamous cell carcinoma.[4] Furthermore, the GPC1 overexpression has been reported in gliomas, lung squamous cell carcinoma (LSCC), breast cancer, prostate cancer, and pancreatic ductal adenocarcinoma (PDAC). In these tumors, a strong correlation between GPC1 overexpression and poor clinical outcomes has been reported [5–9].

Several anti-GPC1 monoclonal antibodies (mAbs) have been developed in both preclinical and clinical studies [10]. A chimeric antibody, Miltuximab, was developed from an anti-GPC1 mAb (clone MIL-38) [10], which was generated by immunization with the UCRU-BL-17CL, a human bladder

 doi:10.20944/preprints202602.1130.v1

cancer cell line [11]. A first-in-human clinical trial of Miltuximab demonstrated its safety and tolerability in patients with advanced PDAC, bladder cancer, and prostate cancer (ACTRN12616000787482) [12]. However, the clinical development of Miltuximab was terminated. Miltuximab has been further developed as an immunotheranostic agent ([^{67}Ga]Ga-DOTA-Miltuximab), and its safety and tolerability have been evaluated in patients with advanced solid tumors[13]. In addition, ^{89}Zr-DFO-Miltuximab has been established as an effective immuno-positron emission tomography imaging probe for the detection of GPC1-positive glioblastoma in mouse models [14]. Radiolabeled Miltuximab, including ^{225}Ac- and ^{177}Lu-labeled forms, has been developed for α- and β-emitting radionuclide therapies, respectively [10,15]. Moreover, a photoimmunotherapy agent, Miltuximab-IR700, has shown a significant reduction in the viability of GPC1-positive cancer cell lines [16].

Beyond these formats, a bispecific T-cell engager, MIL-38-CD3 BiTE, was engineered in a tandem single-chain variable fragment (scFv) configuration by linking the scFv of Miltuximab to an anti-CD3 scFv. This construct effectively redirected T-cell-mediated cytotoxicity toward GPC1-expressing prostate cancer cells in preclinical models [17].

An anti-GPC1 mAb (clone 1-12) exhibited the antitumor efficacy in an esophageal cancer preclinical model via the antibody-dependent cellular cytotoxicity (ADCC) and complement-dependent cytotoxicity (CDC) activity [18]. Furthermore, another anti-GPC1 mAb (clone 01a033) was generated and exhibited a high internalizing activity suitable for antibody–drug conjugates (ADCs) [19,20]. A humanized version of 01a033 (clone T2) was also developed to ADC, which have been evaluated and demonstrated antitumor efficacy in mouse models of gastric cancer, esophageal cancer, glioblastoma, and PDAC [21–23]. Additionally, a dromedary camel VHH nanobody (D4)-based chimeric antigen receptor (CAR) T-cells targeting GPC1 has shown promising antitumor activity in mouse models of PDAC [24].

To target GPC1, our group has developed mAbs against GPC1 (G$_1$Mabs) using flow cytometry-based high-throughput screening. Among 124 clones of G$_1$Mabs, a clone G$_1$Mab-28 (mouse IgG$_1$, κ) specifically recognized GPC1, but not other GPCs in flow cytometry [25]. Therefore, G$_1$Mab-28 possesses potential for tumor therapy. In this study, we isotype-converted G$_1$Mab-28 into G$_1$Mab-28-mG$_{2a}$ (mouse IgG$_{2a}$-type) and G$_1$Mab-28-hG$_1$ (human IgG$_1$-type) and evaluated the ADCC, CDC, and *in vivo* antitumor efficacy against GPC1-positive tumors.

2. Results

2.1. Production of Isotype-Converted mAbs from G$_1$Mab-28

We previously reported that G$_1$Mab-28, an anti-GPC1 mAb, detects GPC1-positive cells by flow cytometry, western blotting, and immunohistochemistry. Furthermore, G$_1$Mab-28 did not show cross-reactivity to other five glypicans (GPC2 to GPC6) in flow cytometry [25]. We next cloned the cDNA of G$_1$Mab-28 and determined the CDR sequences (Figure 1A). Subsequently, a mouse IgG$_{2a}$-type G$_1$Mab-28 (G$_1$Mab-28-mG$_{2a}$) and human IgG$_1$-type G$_1$Mab-28 (G$_1$Mab-28-hG$_1$) were generated by fusing the V$_H$ and V$_L$ CDRs of G$_1$Mab-28 with the C$_H$ and C$_L$ chains of mouse IgG$_{2a}$ and human IgG$_1$, respectively (Figure 1A). A mouse IgG$_{2a}$ isotype control mAb, PMab-231 (referred to as control mIgG$_{2a}$) and a human IgG$_1$ isotype control mAb, humCvMab-62 (referred to as control hIgG$_1$) were also produced. The purity of original and recombinant mAbs was confirmed by SDS-PAGE under reduced condition (Figure 1B). We also confirmed that G$_1$Mab-28-mG$_{2a}$ and G$_1$Mab-28-hG$_1$ reacted with human GPC1-overexpressed Chinese hamster ovary-K1 (CHO/GPC1), but did not cross-react mouse GPC1-overexpressed CHO-K1 (89% sequence identity to human GPC1 [18], Figure 1C) nor CHO-K1 (supplementary Figure 1) in flow cytometry.

Next, the binding affinity of G$_1$Mab-28-mG$_{2a}$ and G$_1$Mab-28-hG$_1$ was determined using flow cytometry. The dissociation constant (K_D) values of G$_1$Mab-28-mG$_{2a}$ and G$_1$Mab-28-hG$_1$ for CHO/GPC1 were determined to be 9.5×10^{-9} M and 1.7×10^{-8} M, respectively (Figure 1D). These

 doi:10.20944/preprints202602.1130.v1

results indicated that G1Mab-28-mG2a and G1Mab-28-hG1 possess higher binding affinity compared to parental mAb, G1Mab-28 as reported previously (K_D: 3.3 × 10^{-8} M) [25].

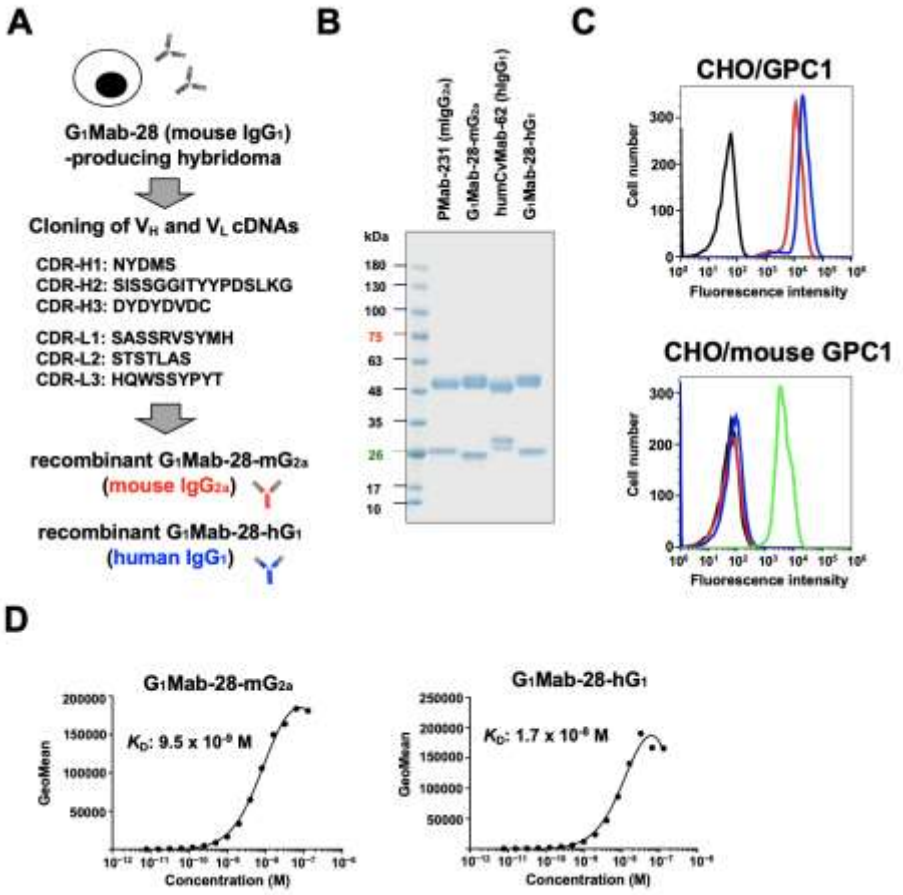

Figure 1. Production of recombinant G1Mab-28-mG2a and G1Mab-28-hG1. (**A**) After determination of CDRs of G1Mab-28 (mouse IgG1), G1Mab-28-mG2a (mouse IgG2a) and G1Mab-28-hG1 (human IgG1) were produced. The amino acid sequence of VH and VL CDRs was indicated. (**B**) PMab-231 (control mIgG2a), G1Mab-28-mG2a, humCvMab-62 (control hIgG1), and G1Mab-28-hG1 were subject to SDS-PAGE, and the gel was stained with Bio-Safe CBB G-250 Stain. (**C**) Flow cytometry using G1Mab-28-mG2a (1 μg/mL; Red line) and G1Mab-28-hG1 (1 μg/mL; Blue line) against CHO/GPC1 and CHO/PA16-mouse GPC1 (CHO/mouse GPC1). An anti-PA16 tag mAb (NZ-1) detected PA16-tagged mouse GPC1 (1 μg/mL; Green line). After treatment with primary mAbs or buffer control (Black line), cells were treated with Alexa Fluor 488-conjugated anti-mouse or rat IgG, or FITC-conjugated anti-human IgG. (**D**) Determination of the binding affinity of G1Mab-28-mG2a and G1Mab-28-hG1 using flow cytometry. CHO/GPC1 was suspended in G1Mab-28-mG2a and G1Mab-28-hG1 at indicated concentrations, followed by Alexa Fluor 488-conjugated anti-mouse IgG or FITC-conjugated anti-human IgG treatment. The SA3800 Cell Analyzer was used to analyze fluorescence data. The dissociation constant (K_D) values were determined using GraphPad Prism 6.

2.2. Flow Cytometry Using G1Mab-28-mG2a and G1Mab-28-hG1 in GPC1-Positive Cancer Cells

We previously screened the GPC1-positive tumor cell lines using flow cytometry. Among them, we chose human LSCC cell lines, such as PC10 and PDAC PK-45H, based on their expression of GPC1 and availability in mouse xenograft models. As shown in Figure 2A and 2B, G1Mab-28-mG2a reacted to PC10 and PK-45H at 1 μg/mL. In contrast, control mIgG2a did not. G1Mab-28-hG1 also showed similar reactivity at 1 μg/mL, but control hIgG1 did not (Figure 2A and 2B). The K_D values of G1Mab-28-mG2a and G1Mab-28-hG1 for PK-45H were determined to be 1.4 × 10^{-9} M and 2.3 × 10^{-9} M, respectively (Figure 2C), indicating that both G1Mab-28-mG2a and G1Mab-28-hG1 exhibit moderate binding affinity to PK-45H.

 doi:10.20944/preprints202602.1130.v1

We next examined GPC1 expression in non-tumor cells. As shown in Figure 2D, G1Mab-28-mG2a and G1Mab-28-hG1 reacted to fibroblast KMST-6, keratinocyte HaCaT, and corneal epithelial hTCEpi.

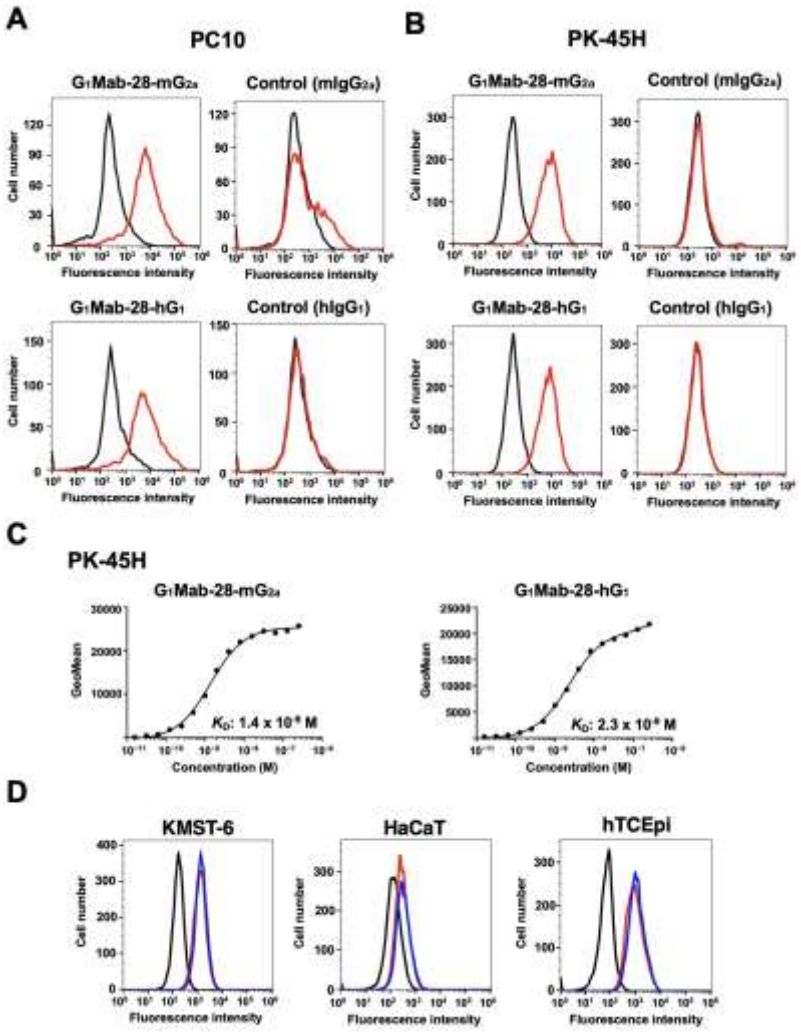

Figure 2. Reactivity of G1Mab-28-mG2a and G1Mab-28-hG1 to tumor cells. (**A, B**) Flow cytometry using control mIgG2a, G1Mab-28-mG2a, control hIgG1, and G1Mab-28-hG1 (1 μg/mL; Red line) or buffer control (Black line) against LSCC PC10 (**A**) and PDAC PK-45H (**B**). After treatment with primary mAbs, cells were treated with Alexa Fluor 488-conjugated anti-mouse IgG or FITC-conjugated anti-human IgG. (**C**) Determination of the binding affinity of G1Mab-28-mG2a and G1Mab-28-hG1 using flow cytometry. PK-45H was suspended in G1Mab-28-mG2a and G1Mab-28-hG1 at indicated concentrations, followed by Alexa Fluor 488-conjugated anti-mouse IgG or FITC-conjugated anti-human IgG treatment. Fluorescence data were analyzed using the SA3800 Cell Analyzer. The dissociation constant (K_D) values were determined using GraphPad Prism 6. (**D**) Flow cytometry using control G1Mab-28-mG2a (1 μg/mL; Red line), G1Mab-28-hG1 (1 μg/mL; Blue line), or buffer control (Black line) against HaCaT, KMST-6, and or TCEpi. After treatment with primary mAbs, cells were treated with Alexa Fluor 488-conjugated anti-mouse IgG or FITC-conjugated anti-human IgG.

2.3. G1Mab-28-mG2a Elicited ADCC and CDC Against GPC1-Positive Cells

ADCC and CDC induced by G1Mab-28-mG2a against GPC1-positive CHO/GPC1, PC10, and PK-45H cells were investigated. The ADCC induced by G1Mab-28-mG2a was evaluated in the presence of effector splenocytes derived from BALB/c nude mice compared with control mIgG2a. As shown in Figure 3A, G1Mab-28-mG2a elicited potent ADCC against CHO/GPC1 (36.7% cytotoxicity; $p < 0.05$) compared with the control mIgG2a (11.5% cytotoxicity). G1Mab-28-mG2a induced ADCC against PC10 (31.8% cytotoxicity; $p < 0.05$) more effectively than the control mIgG2a (11.8% cytotoxicity).

 doi:10.20944/preprints202602.1130.v1

Furthermore, G1Mab-28-mG2a also induced ADCC against PK-45H (31.1% cytotoxicity; $p < 0.05$) more effectively than the control mIgG2a (11.1% cytotoxicity).

The CDC elicited by G1Mab-28-mG2a and complements was next evaluated. As shown in Figure 3B, G1Mab-28-mG2a induced significant CDC against CHO/GPC1 (44.9% cytotoxicity; $p < 0.01$) compared to the control mIgG2a (21.3% cytotoxicity). G1Mab-28-mG2a also elicited CDC against PC10 (12.0% cytotoxicity; $p < 0.05$) more effectively than the control mIgG2a (5.8% cytotoxicity). Additionally, G1Mab-28-mG2a showed CDC against PK-45H (12.3% cytotoxicity; $p < 0.05$) more effectively than the control mIgG2a (4.9% cytotoxicity).

These results indicated that G1Mab-28-mG2a exerted ADCC and CDC in the presence of effector splenocytes and complements, respectively.

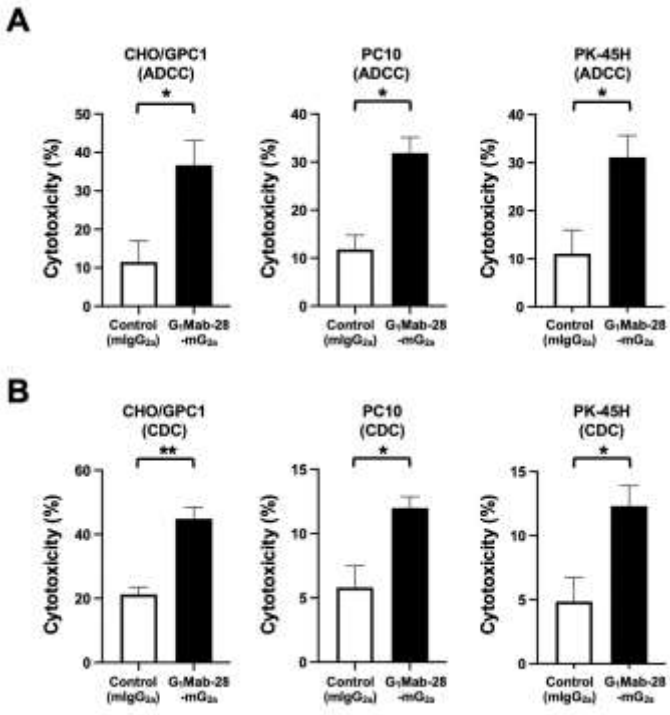

Figure 3. ADCC and CDC by G1Mab-28-mG2a against GPC1-positive tumor cells. The target cells labeled with Calcein AM (CHO/GPC1, PC10, and PK-45H) were incubated with effector splenocyte derived from BALB/c nude mice (**A**) or rabbit complement (**B**) in the presence of G1Mab-28-mG2a or control mIgG2a. Calcein release into the medium was measured, and cytotoxicity was determined. Values are shown as the mean ± SEM. Asterisks indicate statistical significance (* $p < 0.05$, ** $p < 0.01$; two-tailed unpaired t-test).

2.4. G1Mab-28-mG2a Showed Antitumor Effects Against GPC1-Positive Tumor Xenografts

CHO/GPC1, PC10, or PK-45H were inoculated at the left flanks of BALB/c nude mice (day 0). Subsequently, G1Mab-28-mG2a or control mIgG2a was intraperitoneally administered into the tumor-bearing mice on days 7 and 13. The tumor volume was measured on the indicated days. The G1Mab-28-mG2a administration resulted in a significant reduction in CHO/GPC1 xenografts on days 17 ($p < 0.01$) and 20 ($p < 0.01$) compared with that of control mIgG2a (Figure 4A). In the PC10 tumor, a significant reduction was observed on day 17 ($p < 0.01$) and 20 ($p < 0.01$) (Figure 4B). In the PK-45H tumor, a significant reduction was also observed on days 20 ($p < 0.01$) (Figure 4C).

In the tumor weight, G1Mab-28-mG2a showed the potent reduction in CHO/GPC1 (80% reduction; $p < 0.01$; Figure 4D), PC10 (52% reduction; $p < 0.01$; Figure 4E), and PK-45H (39% reduction; $p < 0.01$; Figure 4F) compared with control mIgG2a. The resected CHO/GPC1, PC10, and PK-45H tumors on day 20 are shown in each figure. The tumor-bearing mice did not lose body weight by G1Mab-28-mG2a treatment (Figure 4G–I).

 doi:10.20944/preprints202602.1130.v1

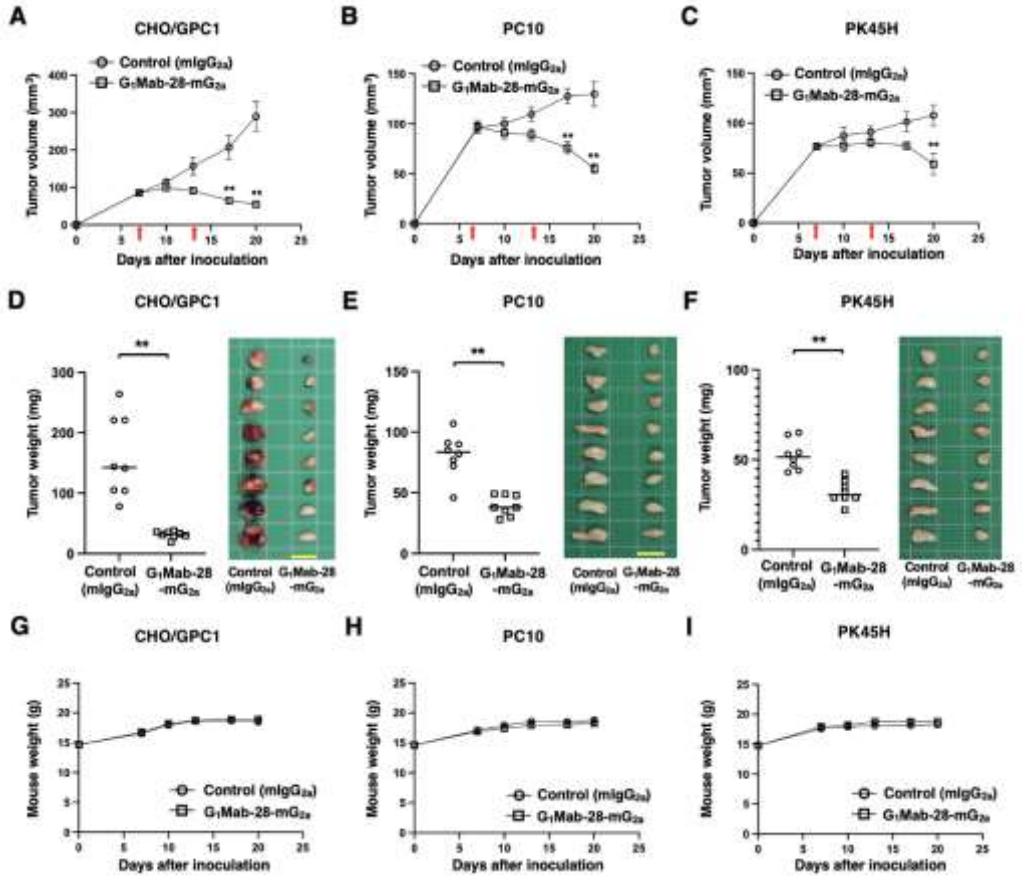

Figure 4. Antitumor activity of G1Mab-28-mG2a against human tumor xenografts. (**A–C**) CHO/GPC1 (**A**), PC10 (**B**), and PK-45H (**C**) cells were subcutaneously injected into BALB/c nude mice (day 0). G1Mab-28-mG2a (100 μg) or control mIgG2a (100 μg) were intraperitoneally injected into each mouse on days 7 and 13 (arrows). The tumor volume is represented as the mean ± SEM. ** $p < 0.01$ (two-way ANOVA with Sidak's post hoc test). (**D–F**) After cell inoculation, the mice were euthanized on day 20. The tumor weights (left) and appearance (right) of CHO/GPC1 (**D**), PC10 (**E**), and PK-45H (**F**) xenografts were measured. Values are presented as the mean ± SEM. ** $p < 0.01$ (two-tailed unpaired t-test). Scale bar, 1 cm. (**G-I**) Body weight (mean ± SEM) of xenograft-bearing mice treated with the mAbs is presented. There is no significant difference (two-way ANOVA with Sidak's post hoc test).

2.5. G1Mab-28-hG1 Elicited ADCC and CDC Against GPC1-Positive Cells

ADCC and CDC induced by G1Mab-28-hG1 against CHO/GPC1, PC10, and PK-45H cells were next investigated. Since all four mouse Fcγ receptors bind to human IgG1 and can elicit ADCC in the presence of mouse effectors [26], the BALB/c nude mice-derived splenocytes were also used as effector cells. The ADCC induced by G1Mab-28-hG1 and control hIgG1 was investigated in the presence of effectors. As shown in Figure 5A, G1Mab-28-hG1 induced potent ADCC against CHO/GPC1 (33.7% cytotoxicity; $p < 0.05$) compared to the control hIgG1 (6.7% cytotoxicity). G1Mab-28-hG1 elicited ADCC against PC10 (28.3% cytotoxicity; $p < 0.05$) more effectively than the control hIgG1 (11.1% cytotoxicity). Furthermore, G1Mab-28-hG1 also showed ADCC against PK-45H (28.7% cytotoxicity; $p < 0.05$) more effectively than the control hIgG1 (8.9% cytotoxicity).

The CDC elicited by G1Mab-28-hG1 and complements was next evaluated. As shown in Figure 5B, G1Mab-28-hG1 elicited significant CDC against CHO/GPC1 (42.8% cytotoxicity; $p < 0.05$) compared to the control hIgG1 (19.7% cytotoxicity). G1Mab-28-hG1 induced CDC against PC10 (11.1% cytotoxicity; $p < 0.05$) more effectively than the control hIgG1 (4.7% cytotoxicity). Additionally, G1Mab-28-hG1 showed CDC against PK-45H (8.0% cytotoxicity; $p < 0.05$) more effectively than the control hIgG1 (3.0% cytotoxicity).

 doi:10.20944/preprints202602.1130.v1

These results indicated that G1Mab-28-hG1 exerted ADCC and CDC in the presence of effector splenocytes and complements, respectively.

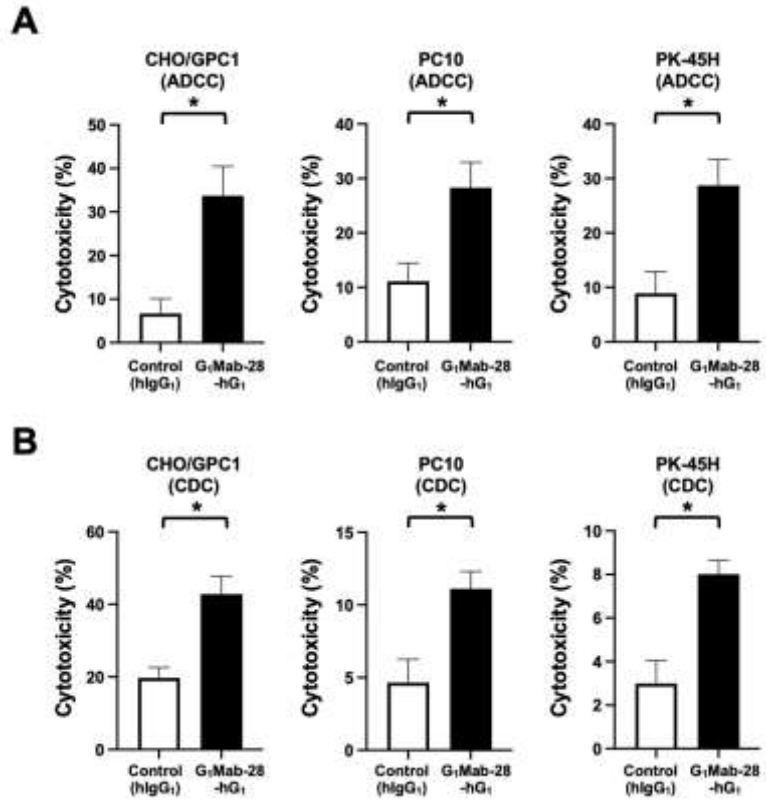

Figure 5. ADCC and CDC by G1Mab-28-hG1 against GPC1-positive tumor cells. The target cells labeled with Calcein AM (CHO/GPC1, PC10, and PK-45H) were incubated with effector splenocyte derived from BALB/c nude mice (**A**) or rabbit complement (**B**) in the presence of G1Mab-28-hG1 or control hIgG1. Calcein release into the medium was measured, and cytotoxicity was determined. Values are shown as the mean ± SEM. Asterisks indicate statistical significance (* $p < 0.05$; two-tailed unpaired *t*-test).

2.6. G1Mab-28-hG1 Showed Antitumor Effects Against GPC1-Positive Tumor Xenografts

In preclinical studies of trastuzumab (human IgG1), a clinically approved anti-HER2 mAb, the antitumor efficacy was evaluated in nude mice in the absence of human-derived effectors [27–29]. Therefore, the antitumor effect of G1Mab-28-hG1 was examined in tumor xenografts inoculated in nude mice. After the inoculation of CHO/GPC1, PC10, or PK-45H in BALB/c nude mice, G1Mab-28-hG1 or control hIgG1 was intraperitoneally administrated into the tumor-bearing mice on days 7 and 13. The G1Mab-28-hG1 administration resulted in a reduction in CHO/GPC1 xenografts on days 17 ($p < 0.01$) and 20 ($p < 0.01$) compared with that of control hIgG1 (Figure 6A). In the PC10 tumor, a significant reduction was observed on day 17 ($p < 0.05$) and 20 ($p < 0.01$) (Figure 6B). In the PK-45H tumor, a significant reduction was also observed on day 20 ($p < 0.01$) (Figure 6C).

In the tumor weight, G1Mab-28-hG1 showed the reduction in CHO/GPC1 (72% reduction; $p < 0.05$; Figure 6D), PC10 (46% reduction; $p < 0.01$; Figure 6E), and PK-45H (41% reduction; $p < 0.01$; Figure 6F) compared with control hIgG1. The resected CHO/GPC1, PC10, and PK-45H tumors on day 20 are shown in each figure. The tumor-bearing mice did not lose body weight by G1Mab-28-hG1 treatment (Figure 6G–I).

 doi:10.20944/preprints202602.1130.v1

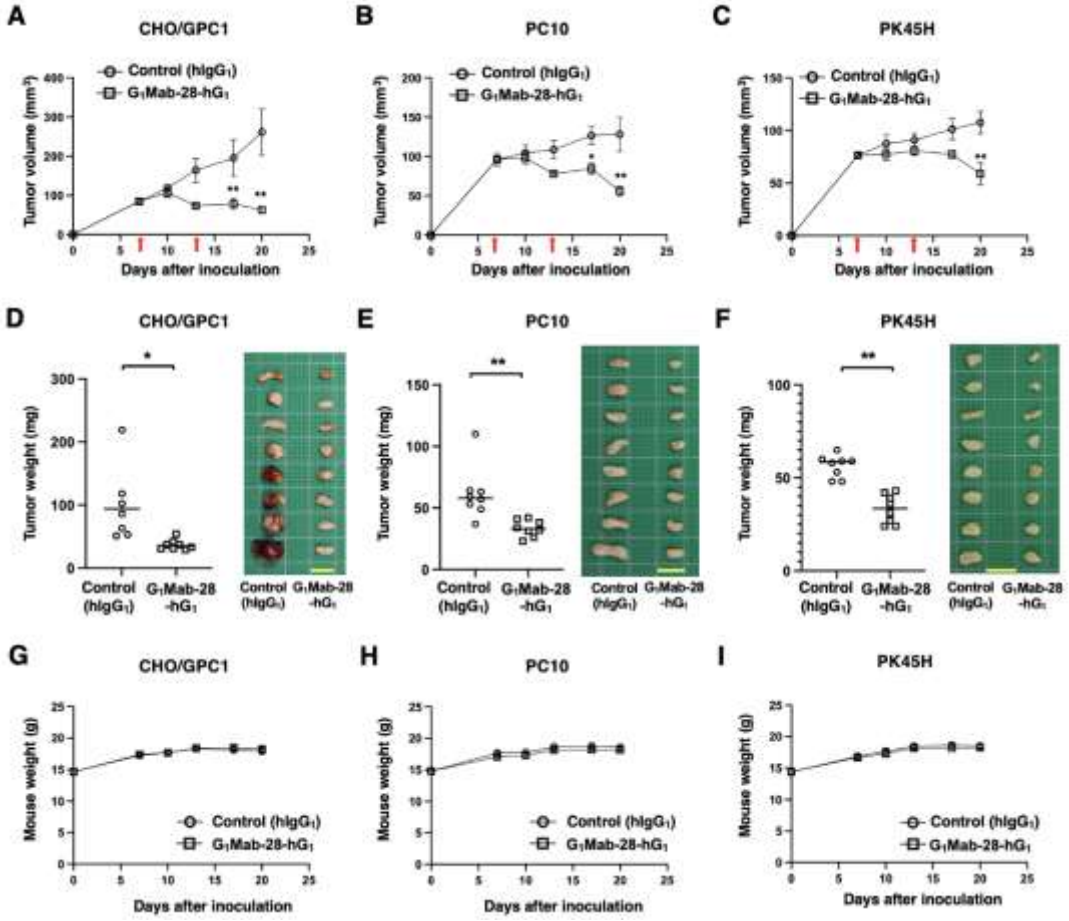

Figure 6. Antitumor activity of G1Mab-28-hG1 against human tumor xenografts. (**A–C**) CHO/GPC1 (**A**), PC10 (**B**), and PK-45H (**C**) cells were subcutaneously injected into BALB/c nude mice (day 0). G1Mab-28-hG1 (100 μg) or control hIgG1 (100 μg) were intraperitoneally injected into each mouse on days 7 and 13 (arrows). The tumor volume is represented as the mean ± SEM. * $p < 0.05$, ** $p < 0.01$ (two-way ANOVA with Sidak's post hoc test). (**D–F**) After cell inoculation, the mice were euthanized on day 20. The tumor weights (left) and appearance (right) of CHO/GPC1 (**D**), PC10 (**E**), and PK-45H (**F**) xenografts were measured. Values are presented as the mean ± SEM. * $p < 0.05$, ** $p < 0.01$ (two-tailed unpaired *t*-test). Scale bar, 1 cm. (**G-I**) Body weight (mean ± SEM) of xenograft-bearing mice treated with the mAbs is presented. There is no significant difference (two-way ANOVA with Sidak's post hoc test).

3. Discussion

This study demonstrated the *in vitro* and *in vivo* antitumor efficacy of a novel mAb against GPC1. Both G1Mab-28-mG2a and G1Mab-28-hG1 recognized CHO/GPC1, PC10, and PK-45H in flow cytometry (Figure 2). In the same experimental setting, the ADCC, CDC (Figure 3 and 5), and *in vivo* antitumor effect (Figure 4 and 6) were observed in G1Mab-28-mG2a and G1Mab-28-hG1. The binding affinity to CHO/GPC1 or PK-45H (Figure 1C and Figure 2D) and the *in vitro*/*in vivo* efficacy (Figure 3-6) were similar between G1Mab-28-mG2a and G1Mab-28-hG1, suggesting that G1Mab-28-hG1 activated the effectors and exerted antitumor efficacy in nude mice.

A chicken/mouse chimeric anti-GPC1 mAb (clone 1-12) exhibited the ADCC and CDC, and inhibited tumor growth of esophageal cancer patient-derived tumor inoculated in SCID or NOD/SCID mice [18]. Since the antitumor effect was observed in severe immunodeficient NOD/SCID mice and the 1-12 were able to detect mouse GPC1 expressed in vascular endothelial cells in tumor microenvironment (TME), the antiangiogenic effect was also thought to be involved in the antitumor effect [18]. In contrast, G1Mab-28-mG2a and G1Mab-28-hG1 did not recognize mouse GPC1 (Figure 1C). Therefore, both mAbs exerted the antitumor effect through the ADCC and CDC mainly.

 doi:10.20944/preprints202602.1130.v1

Furthermore, the reductions of tumor volume were observed at day 20 compared to that at day 7 (treatment start day, Figure 4 and 6), suggesting that the monotherapy of G_1Mab-28-mG_{2a} and G_1Mab-28-hG_1 is expected for tumor treatment.

The above group next developed another anti-GPC1 mAb (clone 01a033) and the humanized version (clone T2), which has a high internalizing activity suitable for ADC [19,20,23]. In PDAC, GPC1 expression was elevated in both PDAC and cancer-associated fibroblasts (CAFs) in 80% of patients [30]. In a mouse xenograft model of PDAC patient-derived tumor with GPC1-positive CAF and tumor cells, the 01a033-ADC showed a potent antitumor effect [30]. These results indicate that targeting GPC1 on PDAC and CAF by the 01a033-ADC is a promising approach in stroma-rich PDAC. For the development of ADC of G_1Mab-28-mG_{2a} and G_1Mab-28-hG_1, the epitope and internalizing activity should be investigated in the future studies.

GPC1 expression in normal tissues has been considered minimal or absent. The distribution of GPC1 in normal tissues has primarily been evaluated by immunohistochemistry (IHC) [31,32]. However, our flow cytometric analyses demonstrated that G_1Mab-28-mG_{2a} and G_1Mab-28-hG_1 recognize fibroblast, keratinocyte, and corneal epithelial cell lines (Figure 2D). As mentioned above, GPC1 was detected in TME, including tumor-infiltrating CAFs and/or vascular endothelial cells [18,30,33]. If anti-GPC1 mAbs act on normal epithelial or stromal cells, this is a concern to apply the modalities to clinical studies. For instance, ocular surface adverse events including dry eye, keratitis/keratopathy, blurred vision, conjunctivitis, and corneal pseudomicrocysts have been attributed to ADC treatment [34,35]. The ideal therapeutic targets are expected to be highly expressed in tumors but no or minimal expression in normal tissues. However, such tumor-associated antigens are limited in their use for the development of therapeutic mAbs.

To achieve a favorable therapeutic index while minimizing on-target toxicity, we have developed cancer-specific monoclonal antibodies (CasMabs) targeting antigens such as podocalyxin, podoplanin, and human epidermal growth factor receptor 2 (HER2) and have successfully identified the corresponding cancer-specific epitopes. An anti-HER2 CasMabs, H_2CasMab-2, was selected from approximately 300 anti-HER2 mAb clones [36]. H_2CasMab-2 selectively recognized HER2 on breast cancer cells but showed no reactivity to normal epithelial cells derived from the mammary gland, kidney proximal tubule, lung bronchus, or colon in flow cytometry [36]. We also revealed the structural basis of the recognition between extracellular domain IV of HER2 and H_2CasMab-2 [37]. Furthermore, a scFv derived from H_2CasMab-2 was incorporated into CAR T cells, which demonstrated cancer-specific reactivity and significant antitumor efficacy in a preclinical study [37]. Currently, the H_2CasMab-2 CAR-T therapy is under evaluation in a phase I clinical trial for patients with HER2-positive advanced solid tumors (NCT06241456). Collectively, these findings highlight the importance of selecting CasMabs against GPC1 and identifying their cancer-specific epitopes as key strategies for the development of therapeutic mAbs and related modalities. We have established 124 clones of GPC1-targeting mAbs and will screen them for cancer-specific reactivity. G_1Mab-28-mG_{2a} and G_1Mab-28-hG_1 will be used as reference antibodies for comparison of antitumor efficacy with anti-GPC1 CasMabs.

Accurate assessment of target expression is essential for determining eligibility for targeted therapies. Evaluation of HER2 by IHC provides a semiquantitative measure of HER2 overexpression in the clinic [38]. Historically, limited attention has been paid to HER2-low tumors. However, the emergence of novel therapeutic agents that require fewer membrane epitopes for clinical efficacy has prompted a reassessment of current IHC protocols with particular emphasis on the lower limits of detection [39]. To facilitate the diagnosis of GPC1-positive tumors, standardization of the IHC protocol is essential. However, in several preclinical studies of anti-GPC1 therapies, polyclonal antibodies have been used to detect GPC1 in formalin-fixed paraffin-embedded (FFPE) tumor sections [19,21–23]. Therefore, an anti-GPC1 mAb suitable for IHC is required. G_1Mab-28 can stain the CHO/GPC1 section using an automated IHC platform [25]. However, G_1Mab-28 was not able to stain the FFPE sections of human tumors, suggesting that conformational changes by antigen retrieval and/or inaccessibility of the mAb may prevent the detection of GPC1 by G_1Mab-28. We have

 doi:10.20944/preprints202602.1130.v1

screened the clones that are suitable for IHC to detect GPC1 from abovementioned G1Mab clones, which would contribute to the standardization and the development of companion diagnosis for GPC1-positive tumors.

4. Materials and Methods

4.1. Cell Lines

A human lung squamous cell carcinoma cell line PC-10 was purchased from Immuno-Biological Laboratories Co., Ltd. (Gunma, Japan). A human PDAC cell line PK-45H and an embryonic fibroblast cell line KMST-6 were obtained from the Cell Resource Center for Biomedical Research, Institute of Development, Aging and Cancer, Tohoku University (Miyagi, Japan). A human keratinocyte cell line HaCaT was obtained from Cell Lines Service GmbH (Eppelheim, Germany). A human corneal epithelial immortalized cell line hTCEpi was purchased from EVERCYTE (Vienna, Austria). A human GPC1-overexpressed Chinese hamster ovary-K1 (CHO/GPC1) cell line was previously established [25]. These cell lines were cultured as described previously [25,40].

The mouse GPC1 (NM_016696.4) cDNA was obtained from OriGene Technologies, Inc. (Rockville, MD, USA). The mouse GPC1 cDNA was cloned into a pCAG-Ble-ssnPA16 vector. The plasmid was transfected into CHO-K1, and stable transfectants were established by sorting with an anti-PA16 mAb, NZ-1, using a cell sorter.

4.2. Antibodies

To generate recombinant mouse IgG2a-type G1Mab-28 (G1Mab-28-mG2a) and human IgG1-type G1Mab-28 (G1Mab-28-hG1), the V_H and V_L cDNAs of G1Mab-28 (mouse IgG1, κ) were cloned into pCAG-Neo and pCAG-Ble vectors together with the corresponding constant regions of mouse IgG2a [41] and human IgG1 [42], respectively. The antibody expression vectors were transfected into ExpiCHO-S cells using the ExpiCHO Expression System to produce G1Mab-28-mG2a and G1Mab-28-hG1. The PMab-231 (for isotype control mouse IgG2a) [41] and humCvMab-62 (for isotype control human IgG1) [42] were also prepared. All antibodies were purified using Ab-Capcher (ProteNova Co., Ltd., Kagawa, Japan). These mAbs were denatured by SDS sample buffer (Nacalai Tesque, Inc., Kyoto, Japan) containing 2-mercaptoethanol and subject to SDS-PAGE. The gel was stained with Bio-Safe CBB G-250 Stain (Bio-Rad Laboratories, Inc., Berkeley, CA, USA).

4.3. Animals

The animal study for the antitumor efficacy of G1Mab-28-mG2a and G1Mab-28-hG1 was approved by the Institutional Committee for Experiments of the Institute of Microbial Chemistry (Numazu, Japan, approval no. 2025-045), within which the work was undertaken, and that it conforms to the provisions of the Declaration of Helsinki. Humane objectives for euthanasia were established as a loss of original body weight to a point of >25% and/or a maximal tumor size of >3,000 mm^3.

4.4. Flow Cytometry and Determination of Binding Affinity

Cells were harvested using 1 mM ethylenediaminetetraacetic acid in phosphate-buffered saline (PBS). The cells were treated with primary mAbs in blocking buffer (0.1% bovine serum albumin in PBS) for 30 min at 4 °C. Then, the cells were treated with Alexa Fluor 488-conjugated anti-mouse or rat IgG (1:2000; Cell Signaling Technology, Inc., Danvers, MA, USA), or fluorescein isothiocyanate (FITC)-conjugated anti-human IgG (1:2000; Sigma-Aldrich Corp., St. Louis, MO, USA for 30 minutes at 4 °C. Fluorescence data were collected using the SA3800 Cell Analyzer (Sony Corp., Tokyo, Japan) and analyzed with FlowJo software (BD Biosciences, Franklin Lakes, NJ, USA).

Cells were treated with serially diluted primary mAbs. Subsequently, the cells were incubated with Alexa Fluor 488-conjugated anti-mouse IgG (200-fold dilution) for 30 minutes at 4 °C. Data were collected using the SA3800 Cell Analyzer, and the geometric mean (GeoMean) was determined with

 doi:10.20944/preprints202602.1130.v1

FlowJo. The dissociation constant (K_D) values were calculated using GraphPad PRISM 6 (GraphPad Software, Inc., La Jolla, CA, USA).

4.5. Antibody-Dependent Cellular Cytotoxicity

Five-week-old female BALB/c nude mice were purchased from Japan SLC, Inc. (Shizuoka, Japan). Effector cells were isolated from the spleens as described previously [43]. Target cells (CHO/GPC1, PC10, and PK-45H) were labeled with 10 μg/mL of Calcein AM (Thermo). The target cells were plated in 96-well plates at a density of 5×10^3 cells/well and combined with effector cells (effector-to-target ratio, 50:1) and 100 μg/mL of either control $mIgG_{2a}$ or G_1Mab-28-mG_{2a}, either control $hIgG_1$ or G_1Mab-28-hG_1. After incubating for 4 hours at 37 °C, the calcein released into the supernatant was measured as described previously [44].

4.6. Complement-Dependent Cytotoxicity

The target cells labeled with Calcein AM (CHO/GPC1, PC10, and PK-45H) were seeded and combined with rabbit complement (final concentration 10%, Low-Tox-M Rabbit Complement; Cedarlane Laboratories, Hornby, ON, Canada) along with 100 μg/mL of either control $mIgG_{2a}$ or G_1Mab-28-mG_{2a}, either control $hIgG_1$ or G_1Mab-28-hG_1. After a 4-hour incubation at 37 °C, the amount of calcein released into the medium was measured as described previously [44].

4.7. Antitumor Activities in Xenografts of Human Tumors

CHO/GPC1, PC10, and PK-45H were mixed with Matrigel Matrix Growth Factor Reduced (BD Biosciences). Subcutaneous injections (5×10^6 cells/mouse) were then given to the left flanks of BALB/c nude mice. On the seventh post-inoculation day, 100 μg of control $mIgG_{2a}$ (n = 8), G_1Mab-28-mG_{2a} (n = 8), control $hIgG_1$ (n = 8), or G_1Mab-28-hG_1 (n = 8) in 100 μL PBS were administered intraperitoneally. Additional antibody injections were given on day 13. The tumor diameter was assessed on days 7, 10, 13, 17, and 20 after the tumor cell implantation. Tumor volume was calculated using the formula: volume = $W^2 \times L/2$, where W represents the short diameter and L the long diameter. The mice's weight was also assessed on days 7, 10, 13, 17, and 20 following tumor cell inoculation. When observations on day 20 were complete, the mice were sacrificed, and tumor weights were assessed after tumor excision.

4.8. Statistical Analyses

The mean ± standard error of the mean (SEM) is presented in all data. A two-tailed unpaired t-test was conducted to measure ADCC, CDC, and tumor weight. ANOVA with Sidak's post hoc test was performed for tumor volume and mouse weight. GraphPad Prism 10 (GraphPad Software, Inc.) was used for all calculations. $p < 0.05$ was considered statistically significant.

Supplementary Materials: The following supporting information can be downloaded at the website of this paper posted on Preprints.org, Figure S1: title; Table S1: title; Video S1: title.

Author Contributions: Conceptualization, M.K.K. and Y.K.; methodology, M.K.K. and T.O.; validation, H. Suzuki. and Y.K.; investigation, H.Y., H.Satofuka, and H. Suzuki.; data curation, H. Suzuki.; writing—original draft preparation, G.L., H.Y. and H.Suzuki.; writing—review and editing, Y.K.; project administration, Y.K.; funding acquisition, H.Satofuka and Y.K. All authors have read and agreed to the published version of the manuscript.

Funding: This research was supported in part by Japan Agency for Medical Research and Development (AMED) under Grant Numbers: JP25am0521010 (to Y.K.), JP25ama121008 (to Y.K.), JP25ama221153 (to Y.K.), JP25ama221339 (to Y.K.), and JP25bm1123027 (to Y.K.), and by the Japan Society for the Promotion of Science (JSPS) Grants-in-Aid for Scientific Research (KAKENHI) grant nos. 24K11652 (to H. Satofuka) and 25K10553 (to Y.K.).

 doi:10.20944/preprints202602.1130.v1

Institutional Review Board Statement: The Institutional Committee for Experiments of the Institute of Microbial Chemistry approved animal experiments (approval no. 2025-045, Approval Date: 11 September, 2025).

Informed Consent Statement: Not applicable.

Data Availability Statement: The data presented in this study are available in the article.

Conflicts of Interest: The authors declare no conflict of interest.

References

1. Tripathi, A.D.; Katiyar, S.; Mishra, A. Glypican1: A potential cancer biomarker for nanotargeted therapy. *Drug Discov Today* **2023**, *28*, 103660, doi:10.1016/j.drudis.2023.103660.
2. Pan, J.; Ho, M. Role of glypican-1 in regulating multiple cellular signaling pathways. *Am J Physiol Cell Physiol* **2021**, *321*, C846-c858, doi:10.1152/ajpcell.00290.2021.
3. Wang, S.; Qiu, Y.; Bai, B. The Expression, Regulation, and Biomarker Potential of Glypican-1 in Cancer. *Front Oncol* **2019**, *9*, 614, doi:10.3389/fonc.2019.00614.
4. Hara, H.; Takahashi, T.; Serada, S.; Fujimoto, M.; Ohkawara, T.; Nakatsuka, R.; Harada, E.; Nishigaki, T.; Takahashi, Y.; Nojima, S.; et al. Overexpression of glypican-1 implicates poor prognosis and their chemoresistance in oesophageal squamous cell carcinoma. *Br J Cancer* **2016**, *115*, 66-75, doi:10.1038/bjc.2016.183.
5. Kai, Y.; Amatya, V.J.; Kushitani, K.; Kambara, T.; Suzuki, R.; Fujii, Y.; Tsutani, Y.; Miyata, Y.; Okada, M.; Takeshima, Y. Glypican-1 is a novel immunohistochemical marker to differentiate poorly differentiated squamous cell carcinoma from solid predominant adenocarcinoma of the lung. *Transl Lung Cancer Res* **2021**, *10*, 766-775, doi:10.21037/tlcr-20-857.
6. Saito, T.; Sugiyama, K.; Hama, S.; Yamasaki, F.; Takayasu, T.; Nosaka, R.; Onishi, S.; Muragaki, Y.; Kawamata, T.; Kurisu, K. High Expression of Glypican-1 Predicts Dissemination and Poor Prognosis in Glioblastomas. *World Neurosurg* **2017**, *105*, 282-288, doi:10.1016/j.wneu.2017.05.165.
7. Duan, L.; Hu, X.Q.; Feng, D.Y.; Lei, S.Y.; Hu, G.H. GPC-1 may serve as a predictor of perineural invasion and a prognosticator of survival in pancreatic cancer. *Asian J Surg* **2013**, *36*, 7-12, doi:10.1016/j.asjsur.2012.08.001.
8. Russell, P.J.; Ow, K.T.; Tam, P.N.; Juarez, J.; Kingsley, E.A.; Qu, C.F.; Li, Y.; Cozzi, P.J.; Martiniello-Wilks, R. Immunohistochemical characterisation of the monoclonal antibody BLCA-38 for the detection of prostate cancer. *Cancer Immunol Immunother* **2004**, *53*, 995-1004, doi:10.1007/s00262-004-0527-7.
9. Matsuda, K.; Maruyama, H.; Guo, F.; Kleeff, J.; Itakura, J.; Matsumoto, Y.; Lander, A.D.; Korc, M. Glypican-1 is overexpressed in human breast cancer and modulates the mitogenic effects of multiple heparin-binding growth factors in breast cancer cells. *Cancer Res* **2001**, *61*, 5562-5569.
10. Ghosh, S.; Huda, P.; Fletcher, N.; Campbell, D.; Thurecht, K.J.; Walsh, B. Clinical development of an anti-GPC-1 antibody for the treatment of cancer. *Expert Opin Biol Ther* **2022**, *22*, 603-613, doi:10.1080/14712598.2022.2033204.
11. Walker, K.Z.; Russell, P.J.; Kingsley, E.A.; Philips, J.; Raghavan, D. Detection of malignant cells in voided urine from patients with bladder cancer, a novel monoclonal assay. *J Urol* **1989**, *142*, 1578-1583, doi:10.1016/s0022-5347(17)39172-3.
12. Gurney, H.; Sabanathan, D.; Gillatt, D.; Poursoultan, P.; Shon, K.H.; Walsh, B.; Velonas, V.; Thurecht, K.; Campbell, D. MILGa-01: A first-in-human study assessing the safety and tolerability of chMIL-38 in metastatic prostate, bladder, and pancreatic cancers. *Journal of Clinical Oncology* **2017**, *35*, e565-e565, doi:10.1200/JCO.2017.35.6_suppl.e565.
13. Sabanathan, D.; Campbell, D.H.; Velonas, V.M.; Wissmueller, S.; Mazure, H.; Trifunovic, M.; Poursoltan, P.; Ho Shon, K.; Mackay, T.R.; Lund, M.E.; et al. Safety and tolerability of Miltuximab(®) - a first in human study in patients with advanced solid cancers. *Asia Ocean J Nucl Med Biol* **2021**, *9*, 86-100, doi:10.22038/aojnmb.2021.55600.1386.
14. Ghosh, S.; Fletcher, N.L.; Huda, P.; Houston, Z.H.; Howard, C.B.; Lund, M.E.; Lu, Y.; Campbell, D.H.; Walsh, B.J.; Thurecht, K.J. Pharmacokinetics and Biodistribution of (89)Zr-Miltuximab and Its Antibody

 doi:10.20944/preprints202602.1130.v1

Fragments as Glypican-1 Targeting Immuno-PET Agents in Glioblastoma. *Mol Pharm* **2023**, *20*, 1549-1563, doi:10.1021/acs.molpharmaceut.2c00760.

15. Yeh, M.C.; Tse, B.W.C.; Fletcher, N.L.; Houston, Z.H.; Lund, M.; Volpert, M.; Stewart, C.; Sokolowski, K.A.; Jeet, V.; Thurecht, K.J.; et al. Targeted beta therapy of prostate cancer with (177)Lu-labelled Miltuximab® antibody against glypican-1 (GPC-1). *EJNMMI Res* **2020**, *10*, 46, doi:10.1186/s13550-020-00637-x.
16. Polikarpov, D.M.; Campbell, D.H.; Lund, M.E.; Lu, Y.; Lu, Y.; Wu, J.; Walsh, B.J.; Zvyagin, A.V.; Gillatt, D.A. The feasibility of Miltuximab®-IRDye700DX-mediated photoimmunotherapy of solid tumors. *Photodiagnosis Photodyn Ther* **2020**, *32*, 102064, doi:10.1016/j.pdpdt.2020.102064.
17. Lund, M.E.; Howard, C.B.; Thurecht, K.J.; Campbell, D.H.; Mahler, S.M.; Walsh, B.J. A bispecific T cell engager targeting Glypican-1 redirects T cell cytolytic activity to kill prostate cancer cells. *BMC Cancer* **2020**, *20*, 1214, doi:10.1186/s12885-020-07562-1.
18. Harada, E.; Serada, S.; Fujimoto, M.; Takahashi, Y.; Takahashi, T.; Hara, H.; Nakatsuka, R.; Sugase, T.; Nishigaki, T.; Saito, Y.; et al. Glypican-1 targeted antibody-based therapy induces preclinical antitumor activity against esophageal squamous cell carcinoma. *Oncotarget* **2017**, *8*, 24741-24752, doi:10.18632/oncotarget.15799.
19. Nishigaki, T.; Takahashi, T.; Serada, S.; Fujimoto, M.; Ohkawara, T.; Hara, H.; Sugase, T.; Otsuru, T.; Saito, Y.; Tsujii, S.; et al. Anti-glypican-1 antibody-drug conjugate is a potential therapy against pancreatic cancer. *Br J Cancer* **2020**, *122*, 1333-1341, doi:10.1038/s41416-020-0781-2.
20. Matsuzaki, S.; Serada, S.; Hiramatsu, K.; Nojima, S.; Matsuzaki, S.; Ueda, Y.; Ohkawara, T.; Mabuchi, S.; Fujimoto, M.; Morii, E.; et al. Anti-glypican-1 antibody-drug conjugate exhibits potent preclinical antitumor activity against glypican-1 positive uterine cervical cancer. *Int J Cancer* **2018**, *142*, 1056-1066, doi:10.1002/ijc.31124.
21. Suzuki, Y.; Serada, S.; Yamashita, M.; Kawabata, K.; Takahashi, T.; Obata, K.; Jo, A.; Funajima, E.; Doki, Y.; Naka, T. Assessing efficacy of anti-glypican-1 antibody-drug conjugate as potential therapeutic approach for gastric cancer. *Gastric Cancer* **2025**, *28*, 1201-1212, doi:10.1007/s10120-025-01647-1.
22. Uchida, S.; Serada, S.; Suzuki, Y.; Funajima, E.; Kitakami, K.; Dobashi, K.; Tamatani, S.; Sato, Y.; Beppu, T.; Ogasawara, K.; et al. Glypican-1-targeted antibody-drug conjugate inhibits the growth of glypican-1-positive glioblastoma. *Neoplasia* **2024**, *50*, 100982, doi:10.1016/j.neo.2024.100982.
23. Munekage, E.; Serada, S.; Tsujii, S.; Yokota, K.; Kiuchi, K.; Tominaga, K.; Fujimoto, M.; Kanda, M.; Uemura, S.; Namikawa, T.; et al. A glypican-1-targeted antibody-drug conjugate exhibits potent tumor growth inhibition in glypican-1-positive pancreatic cancer and esophageal squamous cell carcinoma. *Neoplasia* **2021**, *23*, 939-950, doi:10.1016/j.neo.2021.07.006.
24. Li, N.; Quan, A.; Li, D.; Pan, J.; Ren, H.; Hoeltzel, G.; de Val, N.; Ashworth, D.; Ni, W.; Zhou, J.; et al. The IgG4 hinge with CD28 transmembrane domain improves V(H)H-based CAR T cells targeting a membrane-distal epitope of GPC1 in pancreatic cancer. *Nat Commun* **2023**, *14*, 1986, doi:10.1038/s41467-023-37616-4.
25. Yamamoto, H.; Suzuki, H.; Tanaka, T.; Kaneko, M.K.; Kato, Y. Development of an Anti-Glypican-1 Monoclonal Antibody G1Mab-28 for Flow Cytometry, Western Blotting, and Immunohistochemistry. *Preprints* **2025**, doi:10.20944/preprints202506.0332.v1.
26. Overdijk, M.B.; Verploegen, S.; Ortiz Buijsse, A.; Vink, T.; Leusen, J.H.; Bleeker, W.K.; Parren, P.W. Crosstalk between human IgG isotypes and murine effector cells. *J Immunol* **2012**, *189*, 3430-3438, doi:10.4049/jimmunol.1200356.
27. Pegram, M.; Hsu, S.; Lewis, G.; Pietras, R.; Beryt, M.; Sliwkowski, M.; Coombs, D.; Baly, D.; Kabbinavar, F.; Slamon, D. Inhibitory effects of combinations of HER-2/neu antibody and chemotherapeutic agents used for treatment of human breast cancers. *Oncogene* **1999**, *18*, 2241-2251, doi:10.1038/sj.onc.1202526.
28. Pietras, R.J.; Pegram, M.D.; Finn, R.S.; Maneval, D.A.; Slamon, D.J. Remission of human breast cancer xenografts on therapy with humanized monoclonal antibody to HER-2 receptor and DNA-reactive drugs. *Oncogene* **1998**, *17*, 2235-2249, doi:10.1038/sj.onc.1202132.
29. Baselga, J.; Norton, L.; Albanell, J.; Kim, Y.M.; Mendelsohn, J. Recombinant humanized anti-HER2 antibody (Herceptin) enhances the antitumor activity of paclitaxel and doxorubicin against HER2/neu overexpressing human breast cancer xenografts. *Cancer Res* **1998**, *58*, 2825-2831.

30. Tsujii, S.; Serada, S.; Fujimoto, M.; Uemura, S.; Namikawa, T.; Nomura, T.; Murakami, I.; Hanazaki, K.; Naka, T. Glypican-1 Is a Novel Target for Stroma and Tumor Cell Dual-Targeting Antibody-Drug Conjugates in Pancreatic Cancer. *Mol Cancer Ther* **2021**, *20*, 2495-2505, doi:10.1158/1535-7163.Mct-21-0335.
31. Li, N.; Spetz, M.R.; Ho, M. The Role of Glypicans in Cancer Progression and Therapy. *J Histochem Cytochem* **2020**, *68*, 841-862, doi:10.1369/0022155420933709.
32. Kato, D.; Yaguchi, T.; Iwata, T.; Katoh, Y.; Morii, K.; Tsubota, K.; Takise, Y.; Tamiya, M.; Kamada, H.; Akiba, H.; et al. GPC1 specific CAR-T cells eradicate established solid tumor without adverse effects and synergize with anti-PD-1 Ab. *Elife* **2020**, *9*, doi:10.7554/eLife.49392.
33. Yokota, K.; Serada, S.; Tsujii, S.; Toya, K.; Takahashi, T.; Matsunaga, T.; Fujimoto, M.; Uemura, S.; Namikawa, T.; Murakami, I.; et al. Anti-Glypican-1 Antibody-drug Conjugate as Potential Therapy Against Tumor Cells and Tumor Vasculature for Glypican-1-Positive Cholangiocarcinoma. *Mol Cancer Ther* **2021**, *20*, 1713-1722, doi:10.1158/1535-7163.Mct-21-0015.
34. Lindgren, E.S.; Yan, R.; Cil, O.; Verkman, A.S.; Chan, M.F.; Seitzman, G.D.; Farooq, A.V.; Huppert, L.A.; Rugo, H.S.; Pohlmann, P.R.; et al. Incidence and Mitigation of Corneal Pseudomicrocysts Induced by Antibody-Drug Conjugates (ADCs). *Curr Ophthalmol Rep* **2024**, *12*, 13-22, doi:10.1007/s40135-024-00322-5.
35. Eaton, J.S.; Miller, P.E.; Mannis, M.J.; Murphy, C.J. Ocular Adverse Events Associated with Antibody-Drug Conjugates in Human Clinical Trials. *J Ocul Pharmacol Ther* **2015**, *31*, 589-604, doi:10.1089/jop.2015.0064.
36. Kaneko, M.K.; Suzuki, H.; Kato, Y. Establishment of a Novel Cancer-Specific Anti-HER2 Monoclonal Antibody H(2)Mab-250/H(2)CasMab-2 for Breast Cancers. *Monoclon Antib Immunodiagn Immunother* **2024**, *43*, 35-43, doi:10.1089/mab.2023.0033.
37. Hosking, M.P.; Shirinbak, S.; Omilusik, K.; Chandra, S.; Kaneko, M.K.; Gentile, A.; Yamamoto, S.; Shrestha, B.; Grant, J.; Boyett, M.; et al. Preferential tumor targeting of HER2 by iPSC-derived CAR T cells engineered to overcome multiple barriers to solid tumor efficacy. *Cell Stem Cell* **2025**, *32*, 1087-1101.e1084, doi:10.1016/j.stem.2025.05.007.
38. Rüschoff, J.; Friedrich, M.; Nagelmeier, I.; Kirchner, M.; Andresen, L.M.; Salomon, K.; Portier, B.; Sredni, S.T.; Schildhaus, H.U.; Jasani, B.; et al. Comparison of HercepTest™ mAb pharmDx (Dako Omnis, GE001) with Ventana PATHWAY anti-HER-2/neu (4B5) in breast cancer: correlation with HER2 amplification and HER2 low status. *Virchows Arch* **2022**, *481*, 685-694, doi:10.1007/s00428-022-03378-5.
39. Kang, S.; Kim, S.B. HER2-Low Breast Cancer: Now and in the Future. *Cancer Res Treat* **2024**, *56*, 700-720, doi:10.4143/crt.2023.1138.
40. Tanaka, T.; Suzuki, H.; Ohishi, T.; Kawada, M.; Kaneko, M.K.; Kato, Y. Antitumor Activities by a Humanized Cancer-Specific Anti-Podoplanin Monoclonal Antibody humPMab-117 Against Human Tumors. *Cancer Sci* **2025**, *116*, 2232-2242, doi:10.1111/cas.70103.
41. Kaneko, M.K.; Suzuki, H.; Ohishi, T.; Nakamura, T.; Tanaka, T.; Kato, Y. A Cancer-Specific Monoclonal Antibody against HER2 Exerts Antitumor Activities in Human Breast Cancer Xenograft Models. *Int J Mol Sci* **2024**, *25*, doi:10.3390/ijms25031941.
42. Kaneko, M.K.; Suzuki, H.; Ohishi, T.; Nakamura, T.; Yanaka, M.; Tanaka, T.; Kato, Y. Antitumor Activities of a Humanized Cancer-Specific Anti-HER2 Monoclonal Antibody, humH(2)Mab-250 in Human Breast Cancer Xenografts. *Int J Mol Sci* **2025**, *26*, doi:10.3390/ijms26031079.
43. Ubukata, R.; Ohishi, T.; Kaneko, M.K.; Suzuki, H.; Kato, Y. EphB2-Targeting Monoclonal Antibodies Exerted Antitumor Activities in Triple-Negative Breast Cancer and Lung Mesothelioma Xenograft Models. *Int J Mol Sci* **2025**, *26*, doi:10.3390/ijms26178302.
44. Suzuki, H.; Ohishi, T.; Tanaka, T.; Kaneko, M.K.; Kato, Y. Anti-HER2 Cancer-Specific mAb, H(2)Mab-250-hG(1), Possesses Higher Complement-Dependent Cytotoxicity than Trastuzumab. *Int J Mol Sci* **2024**, *25*, doi:10.3390/ijms25158386.